

ENHANCEMENT OF THE ADSORPTION OF PHENOL RED FROM WASTEWATER ONTO CLINOPTILOLITE BY MODIFICATION WITH N-TERMINATED SILOXANES

REMY M. K. VALA* AND L. TICHAGWA

Department of Chemistry, University of Fort Hare, Private Bag X1314, Alice 5700, Eastern Cape, South Africa

Abstract—The present study investigated the use of local and affordable clinoptilolite for the removal of persistent dyes from water. To improve its adsorption capacity, Na-clinoptilolite was modified chemically with two N-terminated siloxanes (molar mass: 2600 and 11000 g/mol) and used to adsorb the dye phenol red. The results of Fourier-transform infrared spectroscopy (FTIR) showed that N-terminated siloxanes were grafted successfully onto clinoptilolite. Examination by X-ray diffraction and scanning electron microscopy supported the suggestion of modifications observed by FTIR. The modified clinoptilolite showed improved adsorption properties for phenol red: up to 0.32 mg of phenol red were removed per g of clinoptilolite modified with N-terminated siloxanes from water, while HCl-treated clinoptilolite removed only 0.15 mg after 4 h. Langmuir and Freundlich models were used to obtain isotherm parameters. Results (with $R^2 > 0.84$) from pseudo-first and pseudo-second order equations suggested that adsorption could have involved chemisorption and physisorption, probably because of the mineral-organic nature of the materials prepared.

Key Words—Adsorption, Chemical Modification, Clinoptilolite, N-terminated Siloxanes, Phenol Red, Pollutant.

INTRODUCTION

Water pollutants originate from different sources such as domestic sewage, industrial effluents, and farm waste (Mor *et al.*, 2006). Although purification by microorganisms breaks down many organic molecules, those which are persistent have adverse and diverse effects on living organisms (loss of weight, abnormal growth, *etc.*). Dyes are listed among the persistent organic pollutants (Field and Brady, 2003) and are considered as significant pollutants in the environment due to their complex composition, toxicity, mutagenic and carcinogenic properties, poor degradability, and great solubility in water. Not only do dyes affect the aesthetic appearance of water, they can also reduce light penetration and photosynthesis (Kang, 1991; Carmine, 1994; Moldes *et al.*, 2004; García-Montaña *et al.*, 2008; Mittal *et al.*, 2009; Mandal and Bhattacharyya, 2010). Textile industries are one of the major sources of water contamination, accounting for ~15% of the dyes released as waste into the environment (Toor *et al.*, 2006). Besides the textile industries, pigments and other particles are used widely in industries such as leather, paper (ink), food additives and foodstuff, cosmetics, color products, and coating formulations. Dyes polluting most effluents are highly visible even at very low concentrations and may cause significant harm to aquatic biota as well as humans and other animal life.

Even at very low concentrations, dyes are difficult to remove from water by conventional physicochemical and biological methods, such as anaerobic digestion, due to their synthetic origins and their azo-aromatic structure, which render them highly stable and biologically non-degradable (Mishra and Tripathy, 1993; Liu *et al.*, 2010).

Phenol red, 4'-(3 H-2,1-benzoxathiol-3-ylidene) bisphenol, S,S-dioxide, was the pollutant (dye) of interest in the present study. Phenol red can cause irritation to the eyes, respiratory system, and skin, and inhibits the growth of renal epithelial cells (Walsh-Reitz and Toback, 1992). In addition, phenol red is toxic to muscle fibers, and it has been reported to have mutagenic effects (Chung *et al.*, 1981; Baylor and Hollingworth, 1990). Researchers have used bottom ash (from thermal power plants) and deoiled soya (agricultural waste) to remove and recover it from wastewaters. Adsorption capacities of up to 2.6×10^{-5} mol g⁻¹ for bottom ash and deoiled soya adsorbents have been reported (Mittal *et al.*, 2009). Moldes *et al.* (2004) investigated the decolorization of phenol red using laccase from microorganism (*Trametes versicolor*, CBS100.29) growth. Their results were 36% in 24 h and 40% after 48 h. The removal of phenol red on activated charcoal was studied by Iqbal and Ashiq (2007) who found that adsorption was favored at low temperatures, and the dye was chemisorbed on activated charcoal.

Lignocellulosic materials and zeolites (Nethaji and Sivasamy, 2011; Zendejdel *et al.*, 2011) have also been evaluated as adsorbents for the removal of dyes from water effluents. With its honeycomb structure (cavities and/or channels), clinoptilolite is used mainly in the ion exchange of inorganic substances as well as the

* E-mail address of corresponding author:

MVala@ufh.ac.za

DOI: 10.1346/CCMN.2013.0610606

adsorption of light hydrocarbons, such as CH₄, C₂H₆, and C₃H₈ (Aleksandrova *et al.*, 2004; Faghihian *et al.*, 2008). Few reports, however, address the use of clinoptilolite in the removal of organic pollutants from water, even though its feasibility, such as for organosiloxane removal, has been reported (Tsai *et al.*, 1999; Degnan, 2003; Bel'chinskaya *et al.*, 2008). The bond linking the zeolite and the compound used for modification is thought to be between the oxygen atom of the zeolite and an atom of the other moiety, such as the Si atom of a silane (Duval *et al.*, 1994). To the authors' knowledge, no studies have been conducted on the use of N-terminated siloxane for chemical modification of clinoptilolite for adsorption purposes; this is important because nitrogen (with lone pair electrons) bound to clinoptilolite should enhance its adsorption properties, especially toward organic pollutants.

In the present study, batch adsorption was conducted to remove phenol red from aqueous media by HCl-treated clinoptilolite and clinoptilolite chemically modified with N-terminated siloxanes.

METHODS

Siloxanes

Two 3-aminopropyl-terminated polydimethylsiloxanes (Figure 1) of different molecular mass (NH40D, M_m = 2600 g/mol, and NH130D, M_m = 11000 g/mol) were used. Siloxanes were obtained from Wacker Chemie AG (Munich, Germany).

Clinoptilolite treatment

Clinoptilolite pre-treatment. Na-clinoptilolite was obtained from Cape Bentonite (Pty) Ltd, Heidelberg, Western Cape, South Africa. Impurities (cations such as Na⁺, K⁺, Ca²⁺, Mg²⁺, and others) were removed from clinoptilolite according to Barrer and Makki (1964), Elizalde-González *et al.* (2001), Top and Ülkü (2004), and Faghihian and Pirouzi (2009) with slight modifications: 20 g of untreated clinoptilolite were ground into powder in order to pass through a 425 µm USA Standard Testing Sieve (from Fisher Scientific Company, USA). The powder obtained was refluxed in HCl (0.25, 0.5, 1, 2, 5, 8, and 10 N) for 2, 4, and 6 h at 96°C. After filtration (Whatman filter paper, pore size: 20–25µm), the residue was washed thoroughly, first with cold (room temperature) and then with hot (boiling) deionized water, until all traces of acid were removed, and the AgNO₃ chloride test proved negative. The purified

clinoptilolite was then calcinated at 300°C for 8 h in a furnace, and kept for chemical modification. The HCl treated clinoptilolite was designated as "clinop-HCl". Clinoptilolite pre-treated with 0.25 N HCl was found to be best for chemical modification with siloxanes; this deduction was based on the XRD results which revealed the disappearance of the 'broad peak' around 6.85° when the HCl concentration increased, indicating a possible change in the crystallinity or porosity of clinoptilolite. Note that the wide range of HCl concentrations was only used to select the most appropriate concentration for the extraction of impurities but should not affect the clinoptilolite properties.

Chemical modification of clinoptilolite. The pre-treated clinoptilolite was further chemically modified with siloxanes according to the methods of Ban *et al.* (2004): 2.5 g of the 0.25 N HCl pre-treated clinoptilolite was suspended in 80 mL of toluene. After 30 min of stirring, 20 mL of siloxane was added and the mixture was stirred for 24 h at room temperature under N₂. After filtration, the unreacted siloxane was Soxhlet-extracted for 1 h with 80 mL of toluene and then 50 mL of methanol. The modified clinoptilolite was dried for 1 h at 110°C, washed by filtration in deionized water, and oven dried overnight at 65°C. The final products (clinop-NH40D = clinoptilolite modified with siloxane NH40D and clinop-NH130D = clinoptilolite modified with siloxane NH130D) were used as adsorbents.

Experimental procedure for adsorption of phenol red

A phenol red stock solution of 100 mg/L was prepared in de-ionized water and dissolution was achieved through a stainless steel ultrasonicator (from Ningbo Scientz Biotechnology Co., Ltd, Zhejiang-China). All other solutions were prepared from the stock solution. Adsorption experiments were carried out by adding 100 mL solutions of different concentrations (0.25, 0.50, 1.0, 1.5, 2.0 mg/L) of phenol red to 500 mL conical flasks containing 0.1 g of adsorbent (HCl-treated clinoptilolite and clinoptilolite modified with siloxanes) at a pH of 7.1. The flasks were shaken on an orbital shaker (from MRC orbital shaker, Israel) at 160 rpm and at ambient (room) temperature. Aliquots of the shaken solution were taken after 5, 10, 20, 30, 60, 120, 180, 240, 300, and 360 min, filtered through a 0.45 µm Acrodisc® Syringe Filter with Supor® Membrane (from Pall Corporation, USA), and then the phenol red concentrations were measured using UV-Vis spectrophotometer (from Perkin Elmer Lambda 25, Shelton, USA) at 433 nm. The adsorption capacity of the clinoptilolite materials was determined according to the following equation

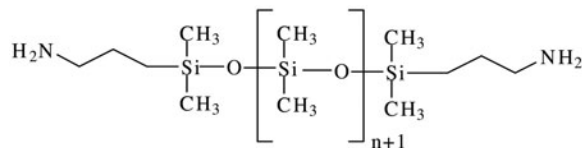


Figure 1. Siloxane structure.

$$Q_t = \frac{V(C_0 - C_t)}{m} \quad (1)$$

where Q_t is the amount of adsorbate adsorbed at time, t ; C_0 is the initial concentration of adsorbate; C_t is the

concentration of adsorbate at time, t ; m is the mass of adsorbent; and V is the volume of adsorbate solution used.

Characterization

All the clinoptilolite materials were characterized by FTIR in a matrix of KBr by means of a Perkin Elmer System 2000 FTIR spectrophotometer (Perkin Elmer, Beaconsfield Bucks, England). X-ray diffraction (XRD) patterns were obtained using a Bruker D8 Advance diffractometer (Bruker, Germany) with $\text{CuK}\alpha$ radiation ($\lambda\text{K}\alpha_1 = 1.5406 \text{ \AA}$) at 40 kV and 40 mA. The surface morphology was examined by scanning electron microscopy (SEM) with a JEOL JSM-6390 LV scanning electron microscope (from JOEL, Tokyo, Japan), using an accelerating voltage of 15 kV.

RESULTS AND DISCUSSION

FTIR of clinoptilolite

The FTIR spectra (Figure 2) were compared to others in the literature (Rusek *et al.*, 2009; Coates, 2000; Mozgawa, 2000; Rivera-Garza *et al.*, 2000; Korkuna *et al.*, 2006; Faghihian *et al.*, 2008; Olad and Naseri, 2010). The peaks at $\sim 3444 \text{ cm}^{-1}$ were ascribed to the vibration of the O–H bonds stretching: the 3552 and 3480 cm^{-1} bands refer to the metallic hydroxides (Al, Mg, Si)–OH, and peaks at 3407 and 1653 cm^{-1} were due to the deformation vibration of the adsorbed water (free or hydration). The peak at $\sim 1042 \text{ cm}^{-1}$ was due to the vibration of the Si–O–Si and asymmetric valence vibrations in the tetrahedral structures of SiO_4 and AlO_4 . The peak at 808 cm^{-1} was due to the symmetrical stretching of AlO_4 for untreated clinoptilolite and to Si–C for the clinoptilolite modified with siloxane (Faghihian *et al.*, 2008).

Low-intensity peaks were observed at 1268 and 2961 cm^{-1} in the spectra of the clinoptilolite modified with siloxanes. These peaks may be attributed to Si–CH₃ and C–H of siloxanes, and represent the grafting of siloxanes onto clinoptilolite.

The results collected here were similar to those in the literature which report two groups of frequencies of vibrations in all zeolites: internal vibrations (considered insensitive to structure) and vibration of external linkages between tetrahedra which are due to the topology and the mode of structure arrangement (Rivera-Garza *et al.*, 2000). The FTIR peaks related to the internal Si–O(Si) and Si–O(Al) vibrations in tetrahedral or aluminato- and silico-oxygen bridges occurred in the range 1200 – 400 cm^{-1} . The peak at 1042 cm^{-1} is due to the Si–O(Si) and Si–O(Al) stretching bands. The peaks due to the presence of zeolite water are at ~ 1600 and 3400 cm^{-1} (Mozgawa, 2000; Katoh *et al.*, 2012).

XRD of clinoptilolite

The effect of HCl treatment on clinoptilolite was studied by XRD. Measurements were made in low (1 – 10) and wide (10 – 52) 2θ angle ranges. The XRD patterns (Figures 3–5) revealed peaks at $6.85^\circ 2\theta$ (broad peak), 9.74° , 22.4° , 26.59° , 27.9° , and 29.9° . In the low-angle range (Figure 3), the broad peak of untreated clinoptilolite at $\sim 6.85^\circ$ was still visible although it was reduced in clinoptilolite treated with HCl.

The reduction of the broad peak was accentuated with acid concentration, until almost no broad peak was observed before the major peak at 9.74° (Figure 4). The disturbance of the Bragg peaks in the low-angle range is probably the result of modification of the crystallinity of clinoptilolite as a consequence of the increase in acid concentration, which might have affected the porosity of the material. Such an effect was reported previously by Kurama *et al.* (2002) (Figure 3).

An important observation during the pre-treatment process was that the color of the clinoptilolite changed from grayish to yellowish after 15 min of reflux with high HCl concentrations (from 0.5 N HCl). That color change was assumed to be due to the removal of surface impurities through degradative reactions, as confirmed by the change in the XRD pattern of the mineral on pre-treatment (Figure 4).

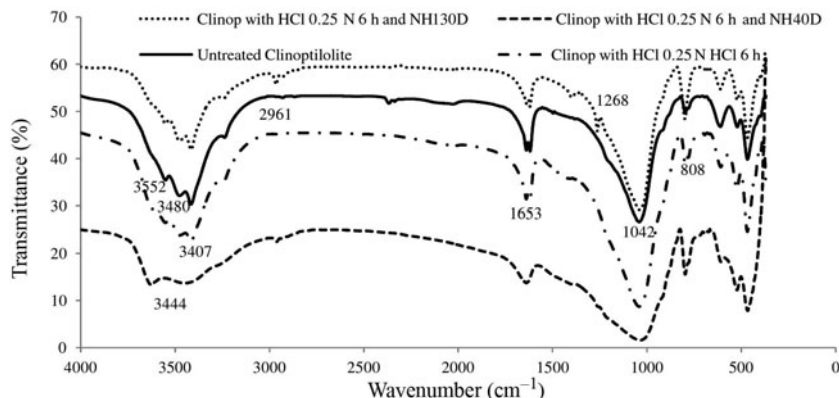


Figure 2. FTIR spectra of untreated, treated, and modified clinoptilolite.

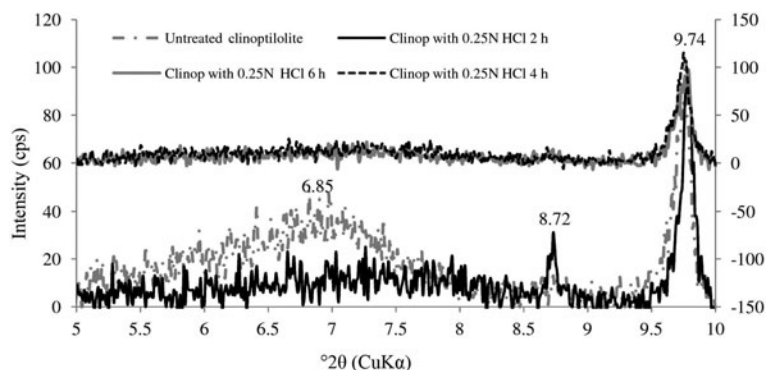


Figure 3. XRD pattern (low-angle range) of clinoptilolite treated with 0.25 N HCl.

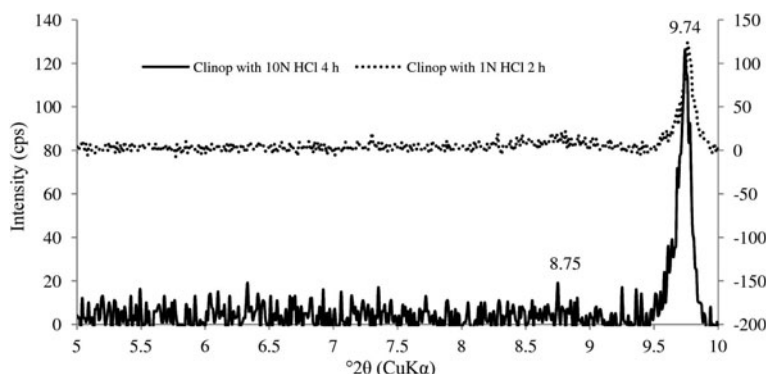


Figure 4. XRD spectra of clinoptilolite treated with concentrations of HCl greater than 0.25 N.

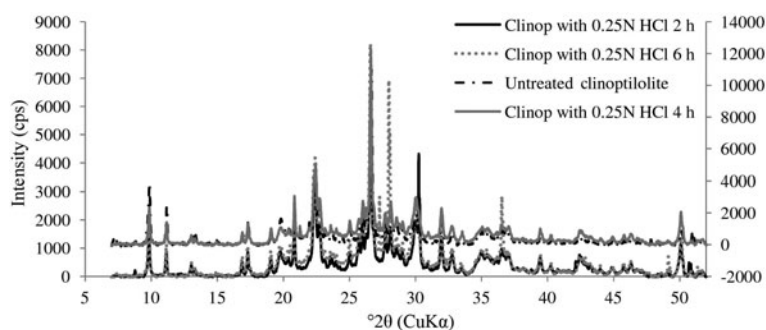


Figure 5. XRD patterns (wide-angle range) of clinoptilolite treated with 0.25 N HCl.

In the wide-angle range (Figure 5), peak positions remained unchanged but their intensities did not. This observation confirmed the disruptive effect of HCl on the crystallinity of the mineral in the low-angle range. Except for the removal of impurities, the concentration of 0.25 N HCl had negligible effects on the crystallinity of clinoptilolite.

The XRD results (low- and wide-angle range) from clinoptilolite modified with siloxanes (Figures 6, 7) revealed that, in the low-angle range, the disappearance of the broad peak previously observed in untreated clinoptilolite shifted from $6.85^{\circ}2\theta$ to $5.42^{\circ}2\theta$. Another important observation was the decrease in peak intensity

(at $9.75^{\circ}2\theta$) from 123 to 40 cps, confirming the presence of siloxanes in the materials.

Although peak intensity decreased (Figure 7), no significant change was observed in the XRD patterns of the materials in the wide-angle range.

SEM of clinoptilolite

The SEM images (Figure 8) showed the difference in the morphology of untreated and treated clinoptilolite. Clinoptilolite treated with HCl showed a more uniform structure than the untreated clinoptilolite, suggesting that the pre-treatment had efficiently removed impurities (cloudiness) from the mineral.

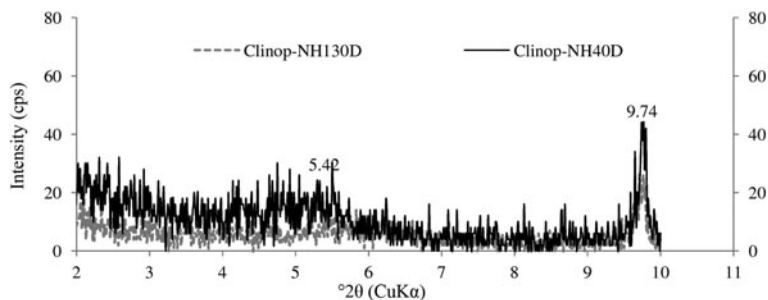


Figure 6. XRD patterns (low-angle range) of clinoptilolite modified with siloxanes.

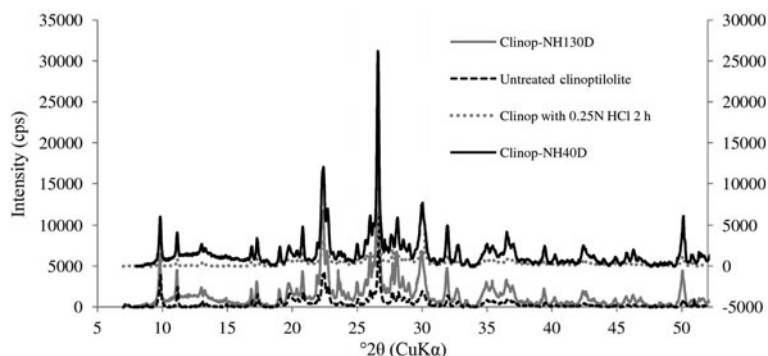


Figure 7. XRD patterns (wide-angle range) of clinoptilolite modified with siloxanes.

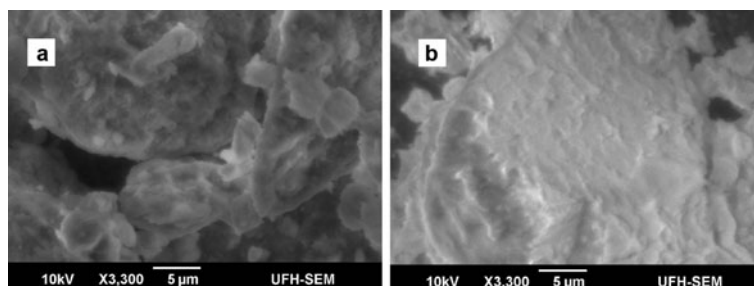


Figure 8. SEM images of clinoptilolite (a) untreated and (b) treated with 0.25 N HCl for 6 h.

Micrographs of clinoptilolite modified chemically with siloxanes are presented in Figure 9. They look cloudy, probably due to the presence of siloxanes bound to clinoptilolite (the bond linking zeolite and siloxane is thought to be between the oxygen atom of the clinoptilolite and the Si atom of the siloxane (Duval *et al.* 1994)) because the unreacted chemicals were removed by Soxhlet extraction during modification. The appearance reflects other reports in the literature (Duval *et al.*, 1994; Aleksandrova *et al.*, 2004; Ban *et al.*, 2004) concerning chemical modification of clinoptilolite with organic compounds.

Adsorption of phenol red

Langmuir and Freundlich isotherms were used to study the adsorption behavior of the clinoptilolite materials. The Langmuir isotherm assumes that the

surface (monolayer and homogeneous) of any adsorbent material contains a number of active sites where the adsorbate attaches itself, that adsorption sites have equal adsorbate affinity, and that adsorption at one site does not affect adsorption at an adjacent site (Vadivelan and Kumar, 2005; Satyawali and Balakrishnan, 2007; Hameed *et al.*, 2007; Sulak *et al.*, 2007; Mohan *et al.*, 2007). The Freundlich isotherm is used to depict heterogeneous systems (Vadivelan and Kumar, 2005; Chatterjee *et al.*, 2007) and neither assumes constant adsorption energy with surface coverage nor predicts a monolayer capacity.

Kinetics (contact time, pseudo-first and pseudo-second order reactions) was used in order to investigate the adsorption process and to explain the sorption mechanism, such as mass transfer and/or chemical reaction. Pseudo-first and pseudo-second order models

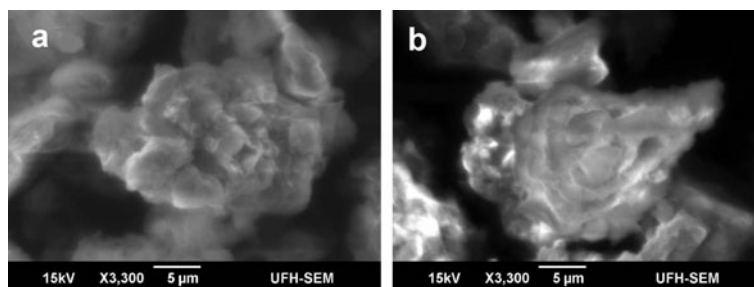


Figure 9. SEM images of clinoptilolite modified with (a) siloxane NH40D and (b) siloxane NH130D.

were used to explain the experimental data. The highest phenol red concentration, 2.0 mg/L, was used to plot adsorption results. Results from other phenol red concentrations showed that adsorption increased with the increase in initial concentration, however.

Effect of contact time and molecular mass on the adsorption of phenol red onto HCl-treated clinoptilolite and clinoptilolite modified with siloxanes. Study of the contact time was helpful in understanding the amount of the dye adsorbed at various time intervals by a fixed amount of the adsorbent. The results (Figure 10) showed the improvement of phenol red uptake on clinoptilolite modified with siloxanes, compared to HCl-treated clinoptilolite. The largest amount of phenol red adsorbed was 0.32 mg/g onto clinop-NH40D. The general adsorption trend could be described as: a sharp increase of phenol red uptake during the first 30 min and then moderate adsorption to equilibrium. Equilibrium was reached after ~120 min for clinop-HCl.

Phenol red uptake continued up to 180 and 240 min for clinop-NH40D and clinop-NH130D, respectively. The presence of siloxanes in the clinoptilolite matrix played a significant role as the adsorption of the dye was improved by a factor of ~2 when compared to clinop-HCl. Although the adsorption capacity of clinoptilolite modified with siloxanes varied slightly, the effect of the molecular mass of siloxanes on the adsorption process showed no significant difference in the correlation

between high molecular mass and adsorption capacities of the adsorbents.

Pseudo-first order and pseudo-second order adsorption of phenol red onto clinoptilolite modified with siloxanes. The rate of adsorption of phenol red onto clinoptilolite modified with siloxanes was also investigated in order to discover whether it fell under pseudo-first or pseudo-second order kinetics. The pseudo-second order model is based on the assumption of chemisorption of the adsorbate on the adsorbent (Ho and McKay, 1999; Srivastava *et al.*, 2006). Linear plots (Figures 11, 12) illustrate the adsorption behaviors of the modified clinoptilolites.

Examination of the correlation coefficients (R^2) of the two models revealed that adsorption was better suited to pseudo-second order than to pseudo-first order because the R^2 for the former (0.9832 and 0.9949 for clinop-NH40D and clinop-NH130D, respectively) was close to unity, suggesting that adsorption could have involved chemisorption (Ho and McKay, 1999; Srivastava *et al.*, 2006). The R^2 values (0.8471 and 0.883 for clinop-NH40D and clinop-NH130D, respectively) obtained by the pseudo-first order model, however, were very good and thus do not exclude the possibility of physisorption.

Isotherms of phenol red adsorbed onto clinoptilolite modified with siloxanes. Adsorption data for phenol red

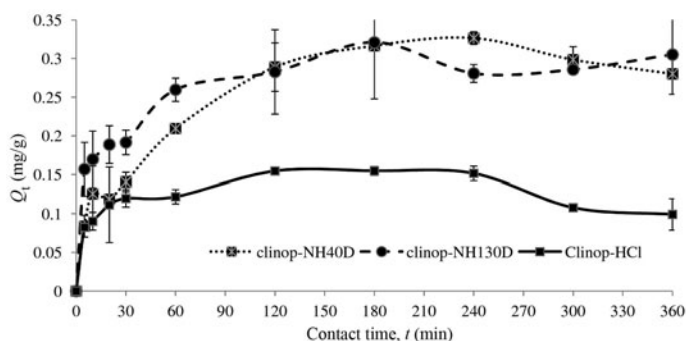


Figure 10. Effect of initial phenol red concentration and contact time on the removal of phenol red by 0.25 N HCl-treated clinoptilolite before and after modification with two different siloxanes (NH40D, NH130D).

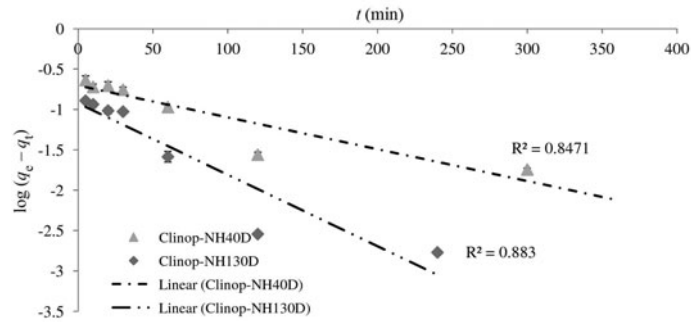


Figure 11. Plots of phenol red-adsorption kinetics for siloxane-modified clinoptilolite using the linear form of the pseudo-first order equation.

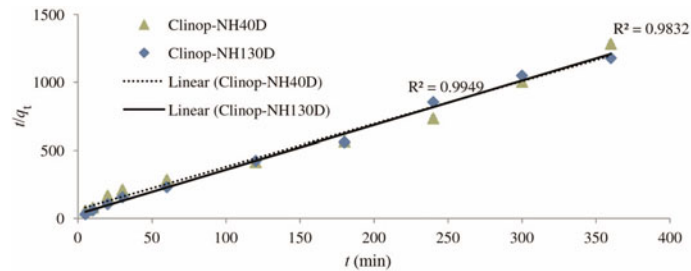


Figure 12. Plots of phenol red-adsorption kinetics for siloxane-modified clinoptilolite using the linear form of the pseudo-second order rate equation.

onto modified clinoptilolites were plotted using linear Langmuir and Freundlich isotherms (Figures 13, 14). Considering the R^2 values of the different plots, adsorption of phenol red onto HCl-treated clinoptilolite and clinoptilolite modified with siloxanes clearly did not fit the Langmuir model (data points are scattered and have small R^2 values), despite the non-negligible value of clinop-NH130D, when compared to the Freundlich model. Consequently, the Freundlich model was assumed to be the better fitting model for adsorption of phenol red onto HCl-treated clinoptilolite and those modified with siloxanes. Many factors could have played an important role in the adsorption of phenol red onto the prepared materials. Interactions which might explain the adsorption mechanism include:

- (1) electrostatic forces that could have been established between the positively charged ketone carrying an additional proton (in the structure of phenol red, which exists as a zwitterion) and the nitrogen of siloxane moiety of the adsorbent;
- (2) H-bond between $-OH$ of phenol red and nitrogen of the adsorbent;
- (3) interactions due to van de Waals forces;
- (4) possible diffusion of the dye into the interior lattice/pores of the adsorbent, and
- (5) $\pi-\pi$ electron donor-acceptor interactions between the aromatic rings of phenol red and the adsorbent.

In the non-linear model (Figure 15), phenol red adsorption onto clinop-NH40D and clinop-NH130D seems to belong to the group VI isotherm, according to Donohue and Aranovich (1998). Their stepwise mechanism represents multilayer adsorption.

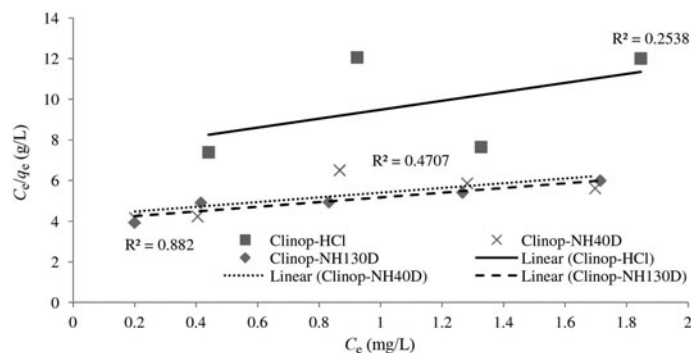


Figure 13. Linear Langmuir isotherms of 0.25 N HCl-treated and siloxane-modified clinoptilolite.

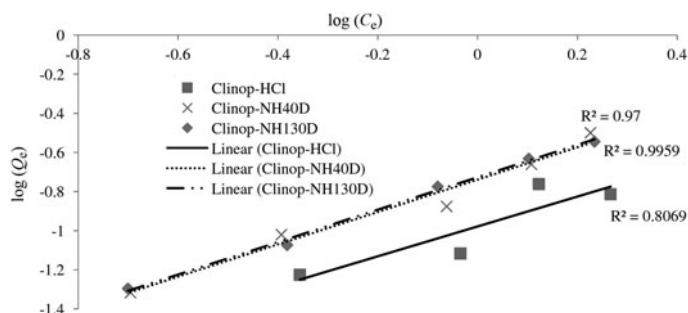


Figure 14. Linear Freundlich isotherms of 0.25 N HCl-treated and siloxane-modified clinoptilolite.

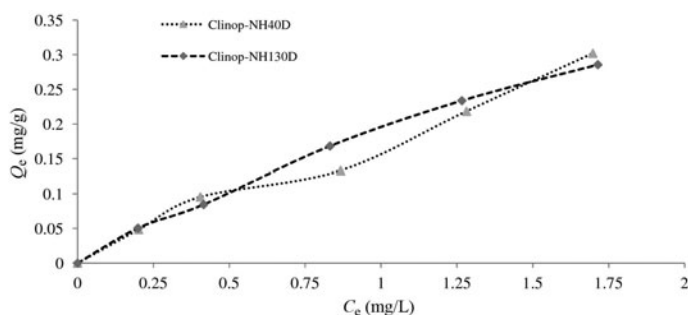


Figure 15. Non-linear isotherms (equation 1) of phenol red adsorbed onto clinoptilolite modified with siloxanes.

CONCLUSIONS

N-terminated siloxanes were grafted onto clinoptilolite after the impurities were removed by a low concentration of HCl solution. The high HCl concentrations had a destructive effect on the crystallinity of clinoptilolite in the low-angle range. To assess the chemical modification of clinoptilolite, which was then used as the adsorbent for phenol red, FTIR, XRD, and SEM were used. Clinoptilolite modified with N-terminated siloxanes showed increased adsorption capacity when compared to clinoptilolite treated with HCl, making these materials good candidates for the removal of dye pollutants from water.

REFERENCES

- Aleksandrova, V.S., Zykova, O.P., and Markiv, E.Ya (2004) Sorption and ion-exchange processes and IR spectra of natural clinoptilolite modified with titanium hydroxo-phosphates. *Russian Journal of Applied Chemistry*, **77**, 30–33.
- Ban, T., Bruehwiler, D., and Calzaferri, G. (2004) Selective modification of the channel entrances of Zeolite L with triethoxysilylated coumarin. *Journal of Physical Chemistry B*, **108**, 16348–16352.
- Barrer, R.M. and Makki, M.B. (1964) Molecular sieve sorbents from clinoptilolite. *Canadian Journal of Chemistry*, **2**, 1481–1487.
- Baylor, S.M. and Hollingworth, S. (1990) Absorbance signals from resting frog skeletal muscle fibers injected with the pH indicator dye, phenol red. *Journal of General Physiology*, **96**, 449–471.
- Bel'chinskaya, L.I., Strel'nikova O. Yu., Novikova, L.A., Ressler, F., and Voishcheva, O.V. (2008) Enhancement of the adsorption selectivity of nanoporous clinoptilolite by hydrophobization with organosiloxanes. *Protection of Metals*, **44**, 390–393.
- Carmine, J.L. (1994) The use of naphthenic acid ester as a dispersing agent in aqueous conductive primers. *Journal of Coatings Technology*, **66**, 93–98.
- Chatterjee, S., Chatterjee, S., Chatterjee, B.P., and Guha, A.K. (2007) Adsorptive removal of Congo Red, a carcinogenic textile dye by chitosan hydrobeads: Binding mechanism, equilibrium and kinetics. *Colloids and Surfaces A*, **299**, 146–152.
- Chung, K.T., Fulk, G.E., and Andrews, A.W. (1981) Mutagenicity testing of some commonly used dyes. *Applied and Environmental Microbiology*, **42**, 641–648.
- Coates, J. (2000) Interpretation of Infrared Spectra: A Practical Approach. Pp. 10815–10837 in: *Encyclopaedia of Analytical Chemistry* (R.A. Meyers, editor). John Wiley & Sons Ltd, New York.
- Degnan, T.F., Jr. (2003) The implications of the fundamentals of shape selectivity for the development of catalysts for the petroleum and petrochemical industries. *Journal of Catalysis*, **216**, 32–46.
- Donohue, M.D. and Aranovich, G.L. (1998) Classification of Gibbs adsorption isotherms. *Advances in Colloid and Interface Science*, **76–77**, 137–152.
- Duval, J.M., Kemperman, A.J.B., Folkers, B., Mulder, M.H.V., Desgrandchamps, G., and Smolders, C.A. (1994) Preparation of zeolite filled glassy polymer membranes. *Journal of Applied Polymer Science*, **54**, 409–418.
- Elizalde-González, M.P., Mattusch, J., Wennrich, R., and Morgenstern, P. (2001) Uptake of arsenite and arsenate by clinoptilolite-rich tuffs. *Microporous and Mesoporous Materials*, **46**, 277–286.
- Faghiani, H. and Pirouzi, M. (2009) Cis/trans-but-2-ene adsorption on natural and modified clinoptilolite. *Clay Minerals*, **44**, 405–409.

- Faghihian, H., Talebi, M., and Pirouzi, M. (2008) Adsorption of nitrogen from natural gas by clinoptilolite. *Journal of the Iranian Chemical Society*, **5**, 394–399.
- Field, J.A. and Brady, J. (2003) Riboflavin as a redox mediator accelerating the reduction of the azo dye mordant yellow 10 by anaerobic granular sludge. *Water Science and Technology*, **48**, 187–193.
- García-Montaña, J., Domènech, X., García-Hortal, J.A., Torrades, F., and Peral, J. (2008) The testing of several biological and chemical coupled treatments for Cibacron Red FN-R azo dye removal. *Journal of Hazardous Materials*, **154**, 484–490.
- Hameed, B.H., Ahmad, A.A., and Aziz, N. (2007) Isotherms, kinetics and thermodynamics of acid dye adsorption on activated palm ash. *Chemical Engineering Journal*, **133**, 195–203.
- Ho, Y.S. and McKay, G. (1999) Pseudo-second order model for sorption processes. *Process Biochemistry*, **34**, 451–465.
- Iqbal, M.J. and Ashiq, M.N. (2007) Adsorption of dyes from aqueous solutions on activated charcoal. *Journal of Hazardous Materials*, **139**, 57–66.
- Kang, H.R. (1991) Water-based ink-jet ink, I. Formulation. *Journal of Imaging Science*, **35**, 179–188.
- Katoh, M., Koide, R., Yamada, K., Yoshida, T., and Horikawa, T. (2012) IR spectroscopic analysis of thermal behavior of adsorbed water on Y-type zeolite. *International Journal of Modern Physics: Conference Series*, **6**, 437–442.
- Korkuna, O., Leboda, R., Skubiszewska-Zięba, J., Vrublevs'ka, T., Gun'ko, V.M., and Ryzkowski, J. (2006) Structural and physicochemical properties of natural zeolites: clinoptilolite and mordenite. *Microporous and Mesoporous Materials*, **87**, 243–254.
- Kurama, H., Zimmer, A., and Reschetilowski, W. (2002) Chemical modification effect on the sorption capacities of natural clinoptilolite. *Chemical Engineering Technology*, **25**, 301–305.
- Mandal, S.S. and Bhattacharyya, A.J. (2010) Titania nanowires as substrates for sensing and photocatalysis of common textile industry effluents. *Talanta*, **82**, 876–884.
- Mishra, G. and Tripathy, M. (1993) A critical review of the treatments for decolourization of textile effluent. *Colourage*, **40**, 35–38.
- Mittal, A., Kaur, D., Malviya, A., Mittal, J., and Gupta, V.K. (2009) Adsorption studies on the removal of coloring agent phenol red from wastewater using waste materials as adsorbents. *Journal of Colloid and Interface Science*, **337**, 345–354.
- Mohan, D., Pittman, C.U., Jr., Bricka, M., Smith, F., Yancey, B., Mohammad, J., Steele, P.H., Alexandre-Franco, M.F., Gómez-Serrano, V., and Gong, H. (2007) Sorption of arsenic, cadmium, and lead by chars produced from fast pyrolysis of wood and bark during bio-oil production. *Journal of Colloid and Interface Science*, **310**, 57–73.
- Moldes, D., Lorenzo, M., and Sanromán, M.Á. (2004) Degradation or polymerisation of Phenol Red dye depending to the catalyst system used. *Process Biochemistry*, **39**, 1811–1815.
- Mor, S., Ravindra, K., Dahiya, R.P., and Chandra, A. (2006) Leachate characterization and assessment of groundwater pollution near municipal solid waste landfill site. *Environmental Monitoring and Assessment*, **118**, 435–456.
- Mozgawa, W. (2000) The influence of some heavy metals cations on the FTIR spectra of zeolites. *Journal of Molecular Structure*, **555**, 299–304.
- Nethaji, S. and Sivasamy, A. (2011) Adsorptive removal of an acid dye by lignocellulosic waste biomass activated carbon: equilibrium and kinetic studies. *Chemosphere*, **82**, 1367–1372.
- Olad, A. and Naseri, B. (2010) Preparation, characterization and anticorrosive properties of a novel polyaniline/c clinoptilolite nanocomposite. *Progress in Organic Coatings*, **67**, 233–238.
- Rivera-Garza, M., Olguin, M.T., García-Sosa, I., Alcantara, D., and Rodríguez-Fuentes, G. (2000) Silver supported on natural Mexican zeolite as an antibacterial material. *Microporous and Mesoporous Materials*, **39**, 431–444.
- Rusek, P., Hubicki, Z., Wójcik, G., and Debczak, A. (2009) Application of the FT-IR/PAS and DRS methods for studying heavy metal ions sorption on the inorganic sorbents. *Acta Physica Polonica A*, **116**, 407–409.
- Satyawali, Y. and Balakrishnan, M. (2007) Removal of color from biometanated distillery spentwash by treatment with activated carbons. *Bioresource Technology*, **98**, 2629–2635.
- Srivastava, V.C., Swamy, M.M., Mall, I.D., Prasad, B., and Mishra, I.M. (2006) Adsorptive removal of phenol by bagasse fly ash and activated carbon: equilibrium, kinetics and thermodynamics. *Colloids and Surfaces A: Physicochemical and Engineering Aspects*, **272**, 89–104.
- Sulak, M.T., Demirbas, E., and Kobya, M. (2007) Removal of Astrazon Yellow 7GL from aqueous solutions by adsorption onto wheat bran. *Bioresource Technology*, **98**, 2590–2598.
- Toor, A.P., Verma, A., Jotschi, , Bajpai, P.K. and Singh, V. (2006) Photocatalytic degradation of Direct Yellow 12 dye using UV/TiO₂ in a shallow pond slurry reactor. *Dyes and Pigments*, **68**, 53–60.
- Top, A. and Ülkü, S. (2004) Silver, zinc, and copper exchange in a Na-clinoptilolite and resulting effect on antibacterial activity. *Applied Clay Science*, **27**, 13–19.
- Tsai, T.C., Liu, S.B., and Wang, I. (1999) Disproportionation and transalkylation of alkylbenzenes over zeolite catalysts. *Applied Catalysis A: General*, **181**, 355–398.
- Vadivelan, V. and Kumar, K.V. (2005) Equilibrium, kinetics, mechanism, and process design for the sorption of methylene blue onto rice husk. *Journal of Colloid and Interface Science*, **286**, 90–100.
- Walsh-Reitz, M.M. and Toback, F.G. (1992) Phenol red inhibits growth of renal epithelial cells. *American Journal of Physiology*, **262**(4 Pt 2), F687–F691.
- Yi, L., Wang, W., and Wang, A. (2010) Removal of Congo Red from aqueous solution by sorption on organified rectorite. *Clean – Soil, Air, Water*, **38**, 670–677.
- Zendehdel, M., Kalateh, Z., and Alikhani, H. (2011) Efficiency evaluation of NaY zeolite and TiO₂/NaY zeolite in removal of methylene blue dye from aqueous solutions. *Iranian Journal of Environmental Health Science & Engineering*, **8**, 265–272.

(Received 17 June 2013; revised 26 October 2013; Ms. 775; AE: S. Kuznicki)